Journal of Biomedical Optics

SPIEDigitalLibrary.org/jbo

Nonlinear microscopy of chitin and chitinous structures: a case study of two cave-dwelling insects

Mihailo D. Rabasović
Dejan V. Pantelić
Branislav M. Jelenković
Srećko B. Ćurčić
Maja S. Rabasović
Maja D. Vrbica
Vladimir M. Lazović
Božidar P. M. Ćurčić
Aleksandar J. Krmpot

SPIE

Nonlinear microscopy of chitin and chitinous structures: a case study of two cave-dwelling insects

Mihailo D. Rabasović,[a] Dejan V. Pantelić,[a,*] Branislav M. Jelenković,[a] Srećko B. Ćurčić,[b] Maja S. Rabasović,[a] Maja D. Vrbica,[b] Vladimir M. Lazović,[a] Božidar P. M. Ćurčić,[b] and Aleksandar J. Krmpot[a]
[a]University of Belgrade, Institute of Physics, Pregrevica 118, 11080 Zemun, Belgrade, Serbia
[b]University of Belgrade—Faculty of Biology, Institute of Zoology, Studentski Trg 16, 11000 Belgrade, Serbia

Abstract. We performed a study of the nonlinear optical properties of chemically purified chitin and insect cuticle using two-photon excited autofluorescence (TPEF) and second-harmonic generation (SHG) microscopy. Excitation spectrum, fluorescence time, polarization sensitivity, and bleaching speed were measured. We have found that the maximum autofluorescence signal requires an excitation wavelength below 850 nm. At longer wavelengths, we were able to penetrate more than 150-μm deep into the sample through the chitinous structures. The excitation power was kept below 10 mW (at the sample) in order to diminish bleaching. The SHG from the purified chitin was confirmed by spectral- and time-resolved measurements. Two cave-dwelling, depigmented, insect species were analyzed and three-dimensional images of the cuticular structures were obtained. © *2015 Society of Photo-Optical Instrumentation Engineers (SPIE)* [DOI: 10.1117/1.JBO.20.1.016010]

Keywords: nonlinear microscopy; fluorescence; two-photon excitation; second-harmonic generation; chitin; insect.

Paper 140595R received Sep. 23, 2014; accepted for publication Dec. 9, 2014; published online Jan. 9, 2015.

1 Introduction

Nonlinear microscopy (NLM) offers a unique insight into a variety of biological structures. Images are generated through multiphoton excited fluorescence, coherent anti-Stokes Raman spectroscopy (CARS), or nonlinear harmonic generation. Tissues and individual cells can be observed with excellent volume details[1]—i.e., lateral resolution is subdiffraction of the order of several hundred nanometers, while the axial resolution is of the order of 2 to 3 μm. This technique is similar to confocal microscopy (in the sense of localized laser excitation and scanning), but with higher penetration depth, less photodamage, and without the need for specimen staining. Up until now, NLM was extensively used in biomedical research, but only marginally in entomology. It is well known that the chitin is a major constituent of the insect's (and arthropod) body and the goal of the study was to investigate the suitability of NLM for deep imaging of chitinous structures. We emphasize the following properties of chitin imaging: higher penetration depth, no need for staining due to efficient autofluorescence of chitin, possibility for *in vivo* imaging, and simultaneous multimodal imaging through harmonics generation.

The insect integument is composed of one live cell layer—epidermis, which produces a complex noncellular outer layer of the integument—cuticle. The cuticle serves as an insect exoskeleton, the site for muscle attachment, and a barrier against predators, parasites, and infection by pathogens.[2] Chitin is the major component of insect cuticle, with addition of proteins (such as resilin, sclerotin, and arthropodin),[3] lipids, waxes, mineral substances, and pigments (papiliochromes, pteridines, ommochromes, melanins, and flavonoids).[4,5] Chitin represents a water-insoluble polysaccharide whose molecules are long-chain sugars consisting of *N*-acetyl-glucosamines bonded with beta-glucosidic linkages.[2] It was extensively studied using a range of techniques: scanning electron microscopy, atomic force microscopy, confocal fluorescent microscopy,[6] transmission electron microscopy,[7] and classical optical microscopy (polarizing interference and transmission).[8]

Traditionally, insect morphology was studied by bright field microscopy. Confocal fluorescence microscopy was also used to observe the structures and organs of insects,[9,10] while two-photon microscopy is still regarded as an emerging technique in entomology. Several papers have been published on the use of NLM in entomology (see Ref. 11 and references within). In Ref. 11, CARS and two-photon excited autofluorescence (TPEF) were used for visualization of *Drosophila melanogaster,* Meigen 1830.

The optical properties of chemically purified chitin have been studied previously. A complex refractive index was investigated in Ref. 12, while its Fourier transform infrared spectra were presented in Ref. 13. Absorption of thin chitin films was investigated in Ref. 14 and two peaks were found. The strong absorption peak was around 330 nm, and the other, much weaker, was identified at 1200 nm. It was found[15] that the fluorescence of the butterfly wings (consisting mostly of chitin) is caused mainly by natural pigments. They are efficiently excited by UV light (at 325-nm wavelength, in the case of various pteridines, 400 nm in papiliochrome, and 340 to 400 nm in melanin[16]). This was used for remote insect monitoring.[17]

Here, we study the nonlinear optical properties of chemically purified chitin and chitinous structures of insects. In the case of chemically purified chitin, we have explored two-photon fluorescence excitation efficiency, fluorescence spectrum, and the bleaching rate. The second-harmonic generation (SHG) was also confirmed. Chitinous structures of two cave-dwelling insect species were analyzed. The insects are adapted for life in underground habitats (troglobites) and belong to two subclasses, Apterygota (wingless insects) and Pterygota (insects with

*Address all correspondence to: Dejan V. Pantelić, E-mail: pantelic@ipb.ac.rs

0091-3286/2015/$25.00 © 2015 SPIE

wings). They are depigmented or have a weak yellow color, transparent, and the cuticle is thinned, with homogeneous chitin.[18] These adaptations allow them to survive in the moisture-saturated atmosphere in caves.[19] By choosing depigmented insects, we largely avoid the fluorescence of pigments (mostly melanin) and other constituents of the insect cuticle.

Cave-dwelling insects, including the two species analyzed herein, are regarded as models for evolution and biogeography, as their reduced aboveground dispersal produces phylogenetic patterns of area distribution that largely matches the geological history of mountain ranges and cave habitats.[20] It should be mentioned that other model organisms have been analyzed using NLM: nematode *Caenorhabditis elegans* (Maupas 1900),[21] as a model in molecular and developmental biologies, and insect *D. melanogaster*[22–24]] as an important model in genetics.

Our results confirm the suitability of two-photon microscopy in entomology as a consequence of high penetration depth, negligible photodamage to the sample, and no need for specimen staining.[25] Measurements and imaging were performed by the homemade NLM with both modalities (TPEF and SHG) enabled.

2 Experimental Setup and Procedures

The experimental setup is shown in Fig. 1. We used two femtosecond lasers to generate two-photon excitation fluorescence and second harmonic images. The Ti-sapphire laser (Coherent Mira 900-F), pumped by a 10-W (Coherent Verdi V10) laser at 532 nm, generates 160-fs pulses at a 76-MHz repetition rate within the 700- to 1000-nm tuning range. We also used a 1040-nm Yb KGW femtosecond laser (Time-Bandwidth Products AG, Yb GLX) as the second excitation source. Galvanometer scanning mirrors (Cambridge Technologies, 6215H) were used to raster-scan the samples. The laser beam was expanded in order to fill the entrance pupil of a microscopic objective. A short-pass dichroic mirror (Thorlabs, DMSP805) directs the laser beam toward the microscopic objective. We were not able to use the full tuning range of the excitation laser due to 805-nm cut-off wavelength of the dichroic mirror. A photomultiplier tube (PMT) (RCA, PF1006) together with an appropriate blocking filter was used for detection of fluorescence and the second harmonic signal. An additional short-pass filter had to be used for the TPEF signal detection in order to reduce the parasitic laser light transmitted through the dichroic mirror. The signal was fed into a 1 MSample/s National Instruments acquisition card (NI USB-6351). The instrument is based on a modified JENAVAL microscopic frame (manufactured by Carl Zeiss). The sample was placed on the existing mechanical stage which was powered by the stepper motor, translating the sample vertically (z-axis in Fig. 1), with a 0.3-μm resolution. Pixel size, z-sectioning step, signal-to-noise ratio (SNR), pixel size, and Nyquist criterion fulfillment depended on the sample itself and on a microscopic objective. The removable prism deflected the beam and enabled the capture of bright field images on a Canon EOS 50D digital camera. The control of the whole instrument and image processing was performed by the computer. VolView 3.4, open-source software (by Kitware, Inc.), was used for three-dimensional (3-D) visualization of a set of slices (either using volume rendering or maximum intensity projection algorithms).

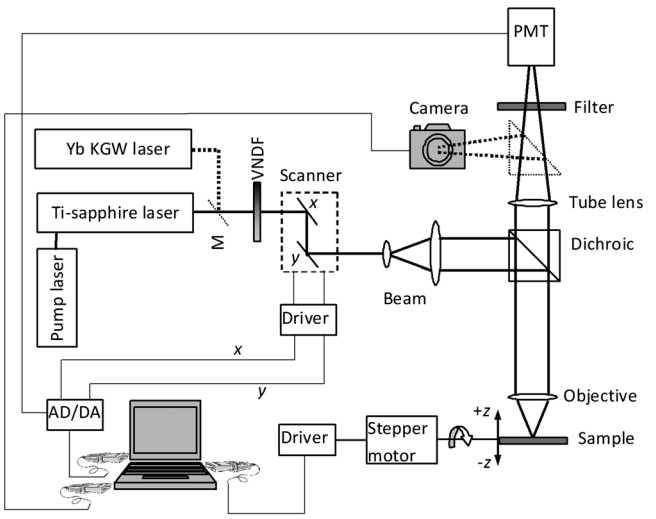

Fig. 1 Scheme of the nonlinear microscope (NLM) experimental setup. PMT is the photomultiplier tube for two-photon excited autofluorescence (TPEF) and second-harmonic generation (SHG) signal detection and VNDF is the variable neutral-density filter for laser power adjustment, while AD/DA is a digital acquisition card. M is a mirror that can be inserted optionally in order to use 1040-nm laser beam from Yb laser. The laser beam path is drawn with thick lines, while electrical wiring is drawn with hair line style.

We mostly used Carl Zeiss objectives: Planachromat, 40×, 0.65 NA (with 815-μm field-of view) and LD LCI Plan-Apochromat 25×, 0.8 NA water/glycerin immersion. For large samples, Carl Zeiss Planachromat, 25×, 0.5 NA (with 1200-μm field-of-view), was used. The lateral and axial resolutions were measured using fluorescently labeled, nanometer-sized beads (Life Technologies, TetraSpeck™ fluorescent microspheres). For the 40× microscopic objective, the lateral resolution was 630 nm by 915 nm (due to the excitation laser-beam ellipticity), while the axial resolution was 2100 nm [full-width at half-maximum (FWHM)].

We used a streak camera (Hamamatsu, C4334) coupled with a spectrograph (Princeton Instruments, SpectraPro 2300i) to study short light pulses due to autofluorescence and SHG. OPO-laser (Opotek, Inc., Vibrant 266-I) was used for single-photon excitation.

Chemically purified chitin and two insects (*Plusiocampa christiani* Condé & Bareth, 1996 and *Pheggomisetes ninae* S. Ćurčić, Schönmann, Brajković, B. Ćurčić & Tomić, 2004) were analyzed. We used commercially available chitin [poly (*N*-acetyl-1,4-β-D-glucopyranosamine] extracted from shrimp shells (Sigma Aldrich, practical grade powder) without further purification. It was used to study the intrinsic fluorescent properties and SHG ability of chitin.

Only natural autofluorescence of the insect specimens was detected. We have selected two depigmented, cave-dwelling species in which the fluorescence of other cuticular components is significantly reduced. This guarantees that the fluorescent signal of chitin is dominant, in contrast to other strongly colored insects.

Plusiocampa christiani is a cave-dwelling, eyeless, and wingless insect belonging to the family Campodeidae, Diplura order. It is endemic to several caves on Kučajske Planine Mts. in Eastern Serbia.[26] As with a majority of cavernicolous invertebrates, this species is without pigments.[27,28] The insect was kept in 70% ethyl alcohol due to its fragility if left to dry. All microscopic observations were done by immersing the insect into glycerin.

Pheggomisetes ninae is a cave-dwelling and blind insect as well, with a pair of coalesced forewings—elytra. Its hind wings are missing. It belongs to the family Carabidae, Coleoptera order. This endemic species inhabits several caves and pits on Mt. Vidlič in Southeastern Serbia.[29] The cuticle of this species is thin as in other troglobitic arthropods, chitinous, almost depigmented, and pale yellow.[30] The genitalia of *P. ninae* males were extracted from the bodies and then kept and observed in glycerin.

Both species prefer wet walls and the floor of caves, where they search for the food, mostly consisting of small invertebrates. They represent typical organisms adapted for life in underground habitats—troglobites. The specimens of both analyzed species are deposited in the collection of the Institute of Zoology, University of Belgrade—Faculty of Biology, Serbia.

3 Autofluorescence and Second-Harmonic Generation Properties of Chemically Purified Chitin

The second harmonic generation (SHG) signal of chemically purified chitin was detected using excitation with ultrashort laser pulses at 1040 nm and an 83-MHz repetition rate from Yb-KGW laser. We use a longer wavelength femtosecond laser in order to significantly reduce the two-photon autofluorescence. The detection system consisted of a streak camera coupled with a spectrograph.

The spectrum of chemically purified chitin exhibits a sharp peak at 520 nm—exactly one half of the excitation wavelength [Fig. 2(a)]. We also measured the temporal response of the signal at 520 nm [see Fig. 2(b)]. It is significantly shorter than the lifetime of TPEF (5.2 ns, as will be shown later) and is equal to the detector response time (approximately 260 ps). This additionally confirms the presence of the second harmonic signal. Two consecutive SHG signal pulses are shown, matching the period between excitation pulses (12 ns).

The intensity of TPEF was measured as a function of the laser wavelength (from 830 to 930 nm) and the laser power (from 3.4 to 13.6 mW at the sample). This particular power range was chosen in order to minimize the photodamage of the biological samples. Figure 3(a) shows that the TPEF signal decreases with the laser wavelength, indicating that the excitation maximum is slightly below 830 nm. Our results were not influenced by the possible spectral dependence of the femtosecond pulse length, because the laser excitation pulses are initially relatively long (more than 160 fs) and insensitive to the operating wavelength, according to the manufacturer. We have always tried to maximize the spectral width of the laser at any particular wavelength, ensuring a constant pulse-width. Dispersion broadening of the optical system is constant and negligible (within the operating wavelength range) compared with the initial pulse-width.[31]

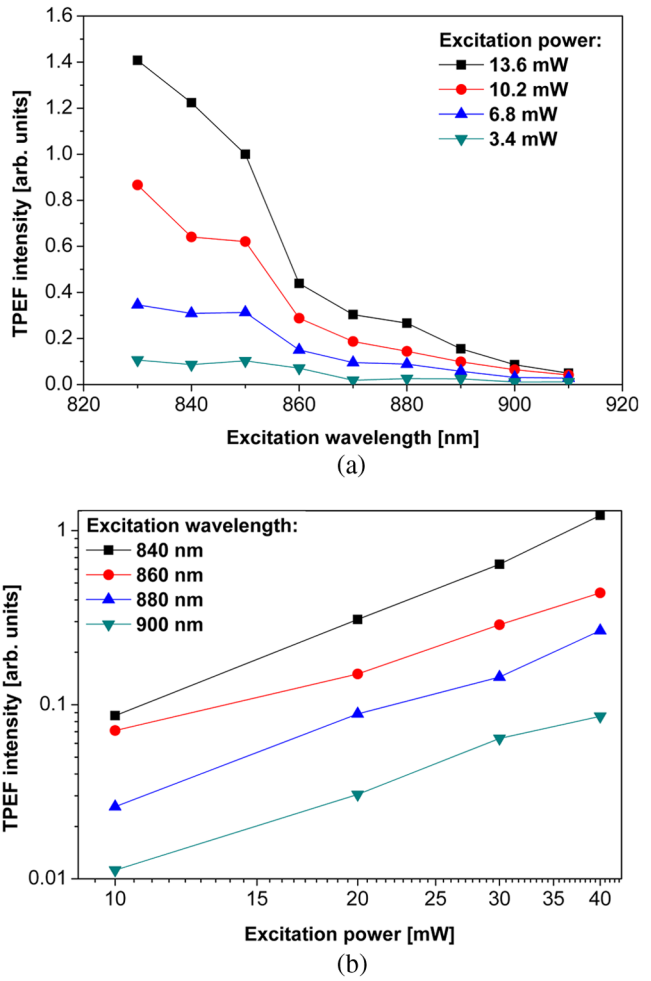

Fig. 3 Intensity of TPEF of chemically purified chitin as a function of (a) laser wavelength (excitation efficiency) and laser power as a parameter; and (b) excitation power (presented in log-log scale) and the laser wavelength as a parameter.

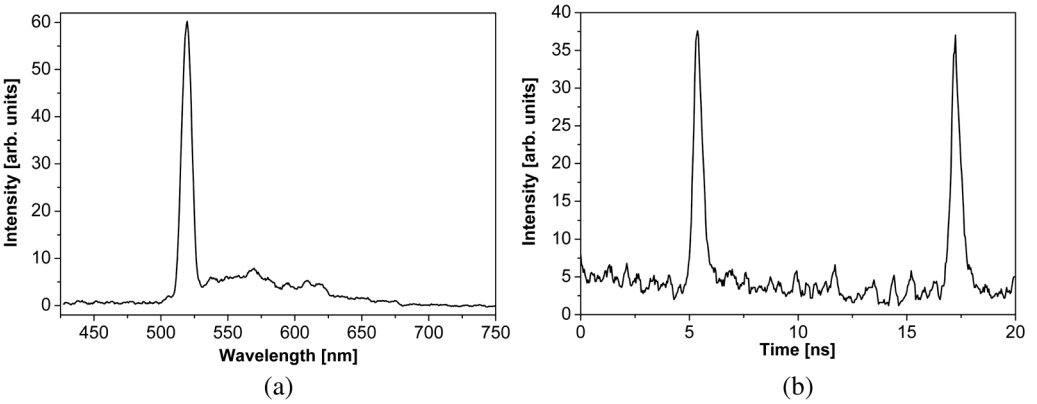

Fig. 2 (a) Spectral and (b) temporal properties of nonlinear response of chemically purified chitin to the excitation by ultrashort pulses at 1040 nm. Pulse repetition rate is 83 MHz.

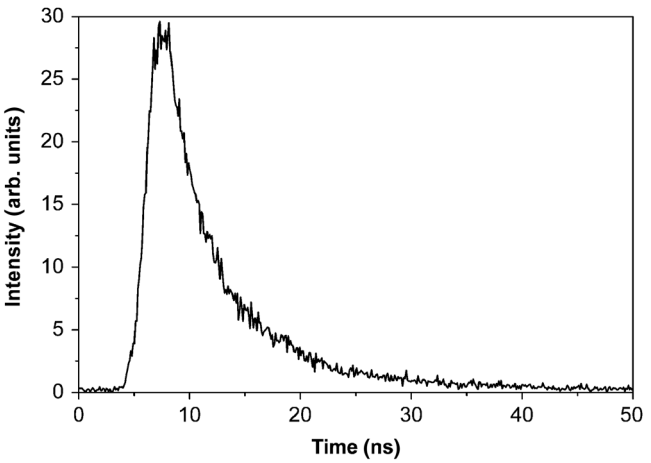

Fig. 4 Fluorescence time of chemically purified chitin.

The intensity of TPEF as a function of excitation power is shown in Fig. 3(b). In order to emphasize the quadratic dependence, the logarithmic scales are chosen on both axes. The two-photon process is exactly quadratic,[32] but we have found the value of the power coefficient to be 1.88 ± 0.05. A slight deviation from the pure quadratic dependence can be explained by a relatively weak TPEF signal and averaging of the signal over a relatively large image area. Increased photobleaching at higher excitation intensities can also play a role in the departure from the quadratic dependence.

In order to measure the fluorescence decay time and the spectrum, we used a single-photon excitation with an OPO-laser and a streak camera coupled with a spectrograph. We have found that the fluorescence decay time of purified chitin is 5.2 ns (Fig. 4), while the fluorescence spectrum has a peak emission at 440 nm and a width of approximately 120 nm (FWHM) (Fig. 5).

We have measured the effects of prolonged irradiation of chitin (both chemically purified and insect) and the corresponding bleaching effects. The focused laser beam irradiated a single spot on a purified chitin sample, and the resulting signal was recorded. The laser power was 70 mW and the corresponding power density was 5.3 MW/cm^2. The decrease in signal intensity is shown in Fig. 6(a). The bleaching effect can be best observed in Fig. 6(b), where a darkened square remained

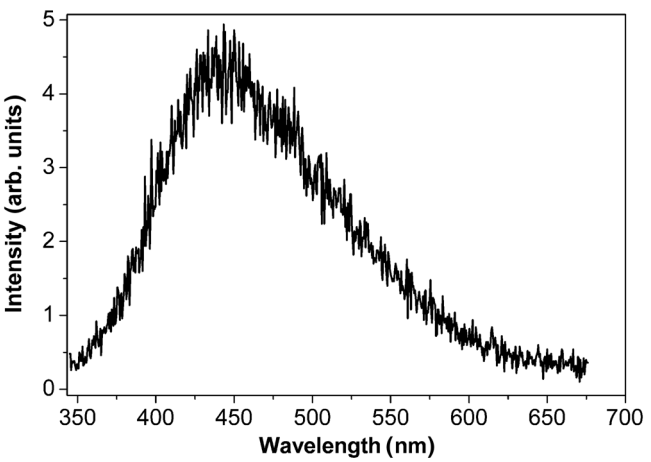

Fig. 5 Autofluorescence spectrum of chemically purified chitin.

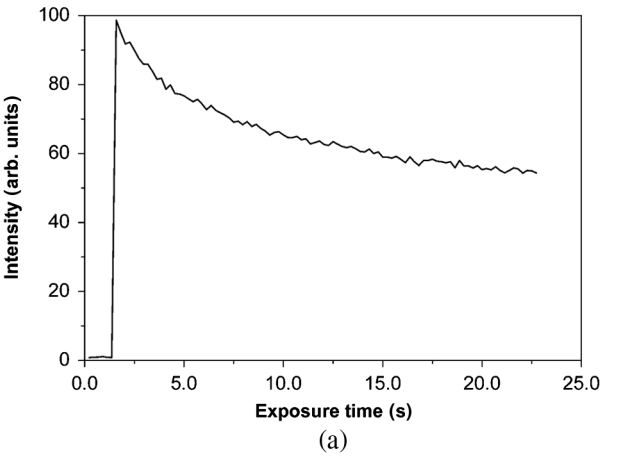

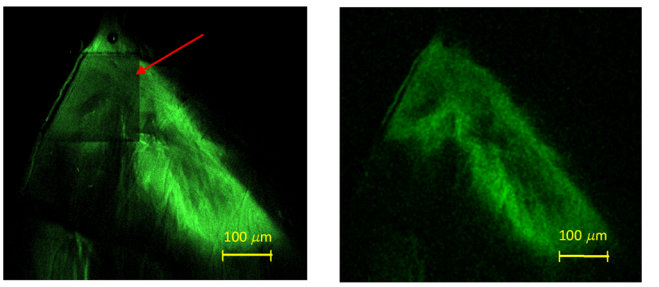

Fig. 6 (a) Decrease of the TPEF signal due to chemically purified chitin photo-bleaching (at 5.3 MW/cm^2 power density). (b) TPEF image of a chitin flake. Prolonged scanning of chemically purified chitin sample produces a rectangular region with reduced fluorescence intensity (red arrow). (c) Bleached square is not visible if sample is imaged using the SHG mode. Both images were taken by 40×/0.65 objective.

after scanning at the higher magnification and 840-nm excitation. If observed using the second-harmonic signal (using narrow band detection filter at 420 nm), the square with reduced intensity could not be detected [Fig. 6(c)]. This is evidence that the purified chitin is not damaged—only its internal structure is permanently modified, diminishing autofluorescence. We have to add that, under normal scanning conditions (high-scanning speed and low-irradiation intensity), bleaching effects are minimal and do not obstruct high-quality image acquisition. Above a certain power level, photodisruption (with plasma formation) was observed. It was highly localized and could be used as another imaging modality.

4 Two-Photon Excited Autofluorescence Microscopy of Cave-Dwelling Insects *Plusiocampa christiani* and *Pheggomisetes ninae*

Here, we present an NLM study of the two cave-dwelling insects: wingless *P. christiani* [Fig. 7(a)] and winged *P. ninae* [Fig. 7(b)]. The data on the morphology and anatomy were given in the descriptions.[26,29] The close correspondence of the evolution and geological record confirms cave-dwelling insects as an important study system for historical biogeography and molecular evolution.[20] They are best suited for testing many hypotheses concerning adaptation strategies during colonization of empty places on Earth.[33] These insects are very precious to the natural biodiversity of the world, because single species can

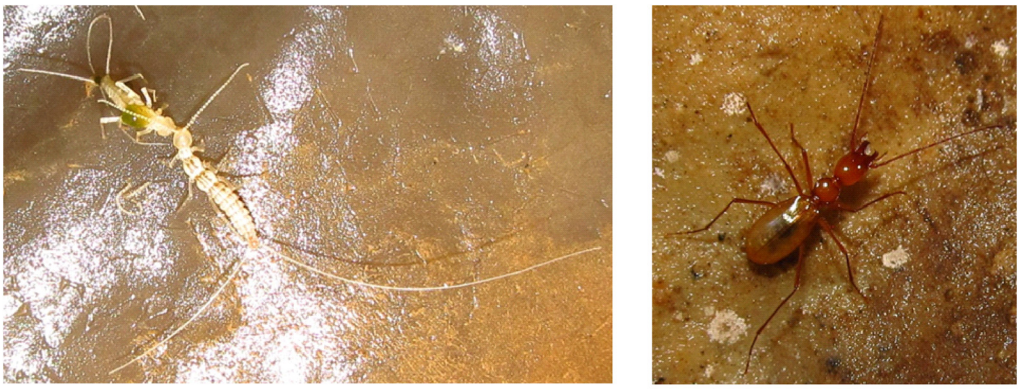

(a) (b)

Fig. 7 (a) *Plusiocampa christiani*; and (b) *Pheggomisetes ninae* (photographs by Dragan Antić).

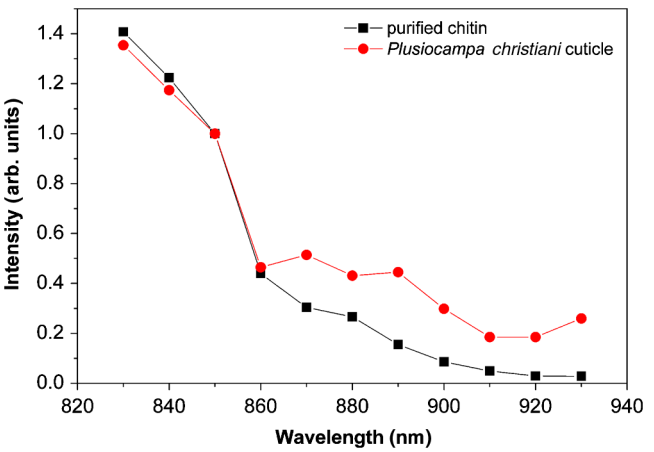

Fig. 8 TPEF spectra of *P. christiani* cuticle and chemically purified chitin.

populate one cave or mountain massif, so the degree of endemism is very high.

Plusiocampa christiani was chosen for its characteristic white appearance which is a consequence of the complete absence of pigments.[28] Apart from a certain amount of proteins, the outer nonliving layer of the insect (cuticle) is regarded as a highly chitinized (sclerotized) structure.[34] The autofluorescent signal comes almost exclusively from chitin, unobscured by the fluorescence of other constituents (i.e., pigments, proteins, and minerals) present in the insects living aboveground. This is supported by the comparison of excitation spectra of *P. christiani* cuticle and chemically purified chitin (Fig. 8). It can be seen that both curves have the same behavior between 830 and 860 nm. At longer wavelengths, the autofluorescence of the insect is higher, signifying the presence of other fluorescent materials in the cuticle (most probably proteins).

We demonstrate the importance of autofluorescence NLM in observing insect morphology by presenting the head of

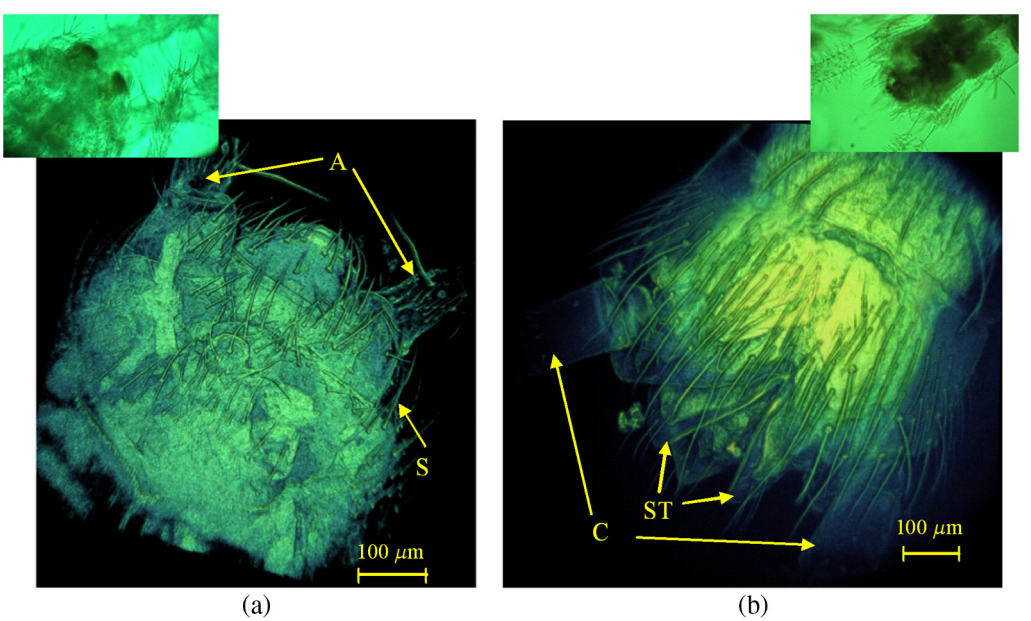

(a) (b)

Fig. 9 TPEF images of *P. christiani*: (a) The head in dorsal view (proximal part of the antennae A and setae S). Field width is 654 μm. (b) The posterior part of the abdomen in dorsal view (proximal part of the cerci C and styli ST). Both three-dimensional (3-D) images were obtained using a maximum intensity projection algorithm (from a set of 80 slices). The images were taken by 40×/0.65 objective. Bright field microscopic images are in insets.

P. christiani in a dorsal view [Fig. 9(a)]. The antennae (seen partially), head sclerites, and sutures can be observed, along with the setation. It is interesting that the mouthparts, situated ventrally, may be seen as well. The laser beam, used to produce a stack of images, had a 12-mW power at the sample. The posterior part of the abdomen of the same insect in the dorsal view is shown in Fig. 9(b). Here, we clearly observe attached paired appendages: multisegmented cerci (seen partially) and shorter styli. The setation and segmentation are well distinguished.

Pheggomisetes ninae is slightly pigmented and its autofluorescence certainly has components stemming both from chitin and other cuticular components. Its apical part of the head in the ventral view is shown in Fig. 10(a), where the mouthparts

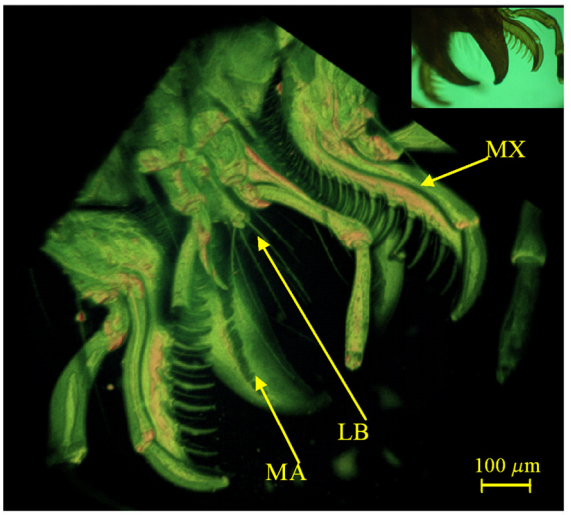

(a)

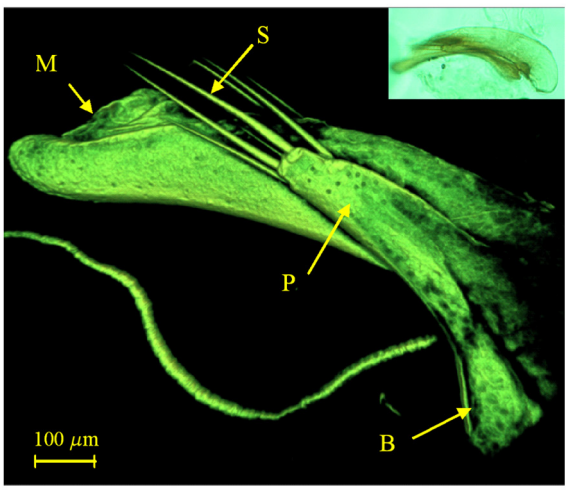

(b)

Fig. 10 Two-photon autofluorescence images of cave-dwelling beetle *P. ninae*: (a) The apical part of the head with mouthparts in ventral view (mandible MA, maxillae MX, and labium LB). The image was taken by 25×/0.5 objective and rendered from a stack of 230 slices using VolView 3.4 (see also accompanying Video 1). (b) The male genitalia in lateral view (median lobe M, parameres P, parameral setae S, and basal bulb B). The image was taken by 40×/0.65 objective and rendered from a stack of 120 slices (see also accompanying Video 2). Bright field microscopic images are in insets. (Video 1, MPEG 7.1 MB) [URL: http://dx.doi.org/10.1117/1.JBO.20.1.016010.1]; (Video 2, MPEG 7.1 MB) [URL: http://dx.doi.org/10.1117/1.JBO.20.1.016010.2].

(mandibles, maxillae, and labium) are very visible, including the fine surface structure and setation.

Images of male genitalia of *P. ninae* are shown in Fig. 10(b). The features of the insect male copulatory organ (aedeagus) are of a great significance in species determination and are usually presented and imaged in taxonomical studies. We used 25× NA 0.8 water/glycerin immersion objective and 930-nm excitation wavelength. Longer wavelengths were used in order to avoid the autofluorescence of residual tissues that remained after insect dissection. At the same time, it was possible to penetrate deeper into the sample through the chitinous cuticle due to the reduced two-photon absorption of chitin. From the lateral view of *P. ninae* aedeagus, a fine relief can be observed on the surface, a complex teeth-like structure of the copulatory piece is visible, and both the inner sac and strongly sclerotized areas of the aedeagus are recognizable (see longitudinal and cross-sections in Figs. 11(a)–11(d)). All mentioned structures are seen in more detail compared with light or confocal microscopy. All parts of the male copulatory organ are well visible and delimited (median lobe, both parameres with the setae, basal bulb, copulatory piece, and inner sac). The penetration depth can be estimated to 200 μm for the given sample [see the scale bar in Fig. 11(b)].

5 Discussion

As shown above, the NLM is a valuable tool for observation of various insect body parts. In the current study, we have chosen cave-dwelling insects in order to separate the fluorescence of chitin from other cuticular components. During experiments, we have investigated a number of other insect species, such as *Apatura ilia* (Denis & Schiffermüller, 1775), *A. iris* (Linnaeus, 1758), and *Pieris rapae* (Linnaeus, 1758) butterflies, and found that each of them produced an autofluorescence signal. Its intensity ranged from good to excellent, depending on the investigated part of the body. The nature of autofluorescence was not always clear, since it depends on the cuticle structure. It is well known that the cuticle is secreted by epidermal cells as thin lamellae or sheets, like sheets of paper stacked on top of each other. The molecules of chitin both from exo- and endocuticles of insect integument can be visualized using multiphoton microscopy in the current study. With TPEF microscopy, even some chitinous structures that are lying beneath the integument (e.g., fine structure of the copulatory piece of the aedeagus) can be observed as well [Fig. 11(d)].

We emphasize that NLM is quite a universal tool, and its range of applicability is by no means limited to any particular insect group. We have found that by choosing the appropriate excitation wavelength (840 to 930 nm or 1040 nm), different components of cuticle could be observed with varying penetration depths. Figure 12 shows the image of the inner sac of *P. ninae* aedeagus, imaged using 1040-nm excitation and broadband detection. By comparing Figs. 11(d) and 12, different structures are emphasized at two wavelengths.

The presence of the second-harmonic signal and the SHG imaging of chitinous structures were barely mentioned in Refs. 35 and 36, but without strong experimental confirmation. In our study, the SHG signal of purified chitin was clearly detected (see Sec. 3), but its intensity was low compared with the autofluorescence. In spite of that, the SHG signal was used to image the naturally occurring chitin of insect cuticle, too. As an example, a part of the antenna of *P. christiani* was imaged under SHG and TPEF conditions (Fig. 13). Images were taken

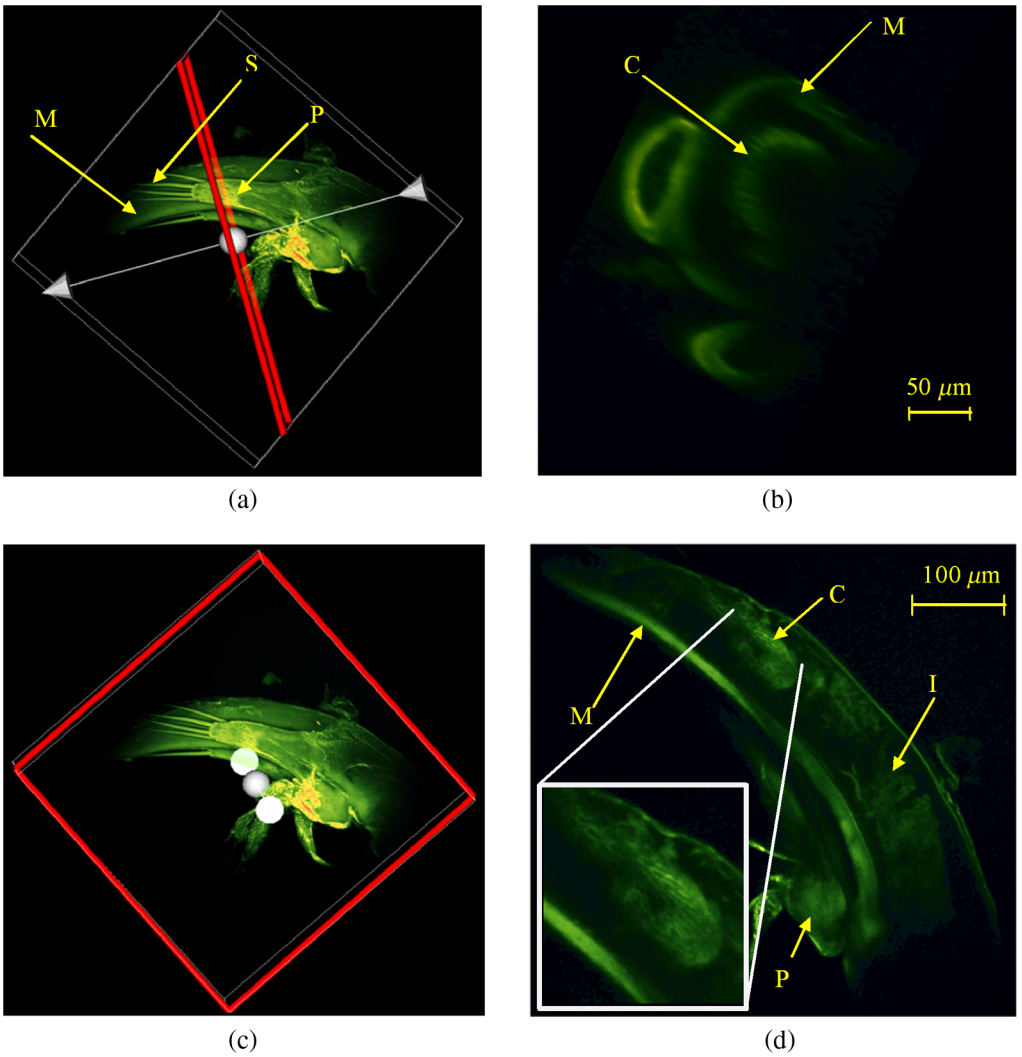

Fig. 11 TPEF images of cave-dwelling beetle *P. ninae*: (a) The male genitalia with cross-sectional plane (red line), median lobe M, parameres P, and parameral setae S. (b) A corresponding cross-section of the genitalia showing median lobe M and copulatory piece C (yellow arrows). (c) The male genitalia with longitudinal section plane (red square). (d) A corresponding longitudinal section of the male genitalia showing the structure of median lobe M, paramere P, inner sac I, and copulatory piece C (yellow arrows). Inset (white square) in (d) is the enlarged copulatory piece with clearly visible teeth-like structure. The images were taken by 25×/0.8 water/glycerin immersion objective.

using 840-nm excitation combined with either broadband [400 to 700 nm, see Fig. 13(a)] or narrowband [420 nm, see Fig. 13(b)] detection filters. From Fig. 13(a), it can be seen that the broadband detection produced fine details of the antenna, while narrow-band SHG conditions produced only an outline. A set of SHG slices was used to construct a 3-D-view of the antenna [Fig. 13(c)]. We emphasize that the SHG signal is much weaker compared with fluorescence which dominates in Fig. 13(a). Therefore, we did not need an additional filter to suppress SHG signal when observing fluorescence.

In order to study the polarization effects, we experimentally confirmed that our detection system is not sensitive to signal polarization. Also, the acquired polarization ellipticity in the excitation arm of the microscope is negligible.

It is well known that the dependence of the detected signal to the polarization state of excitation light may be regarded as a strong indication of the SHG.[37,38] However, we have found that the polarization effects were pronounced both under SHG (840-nm excitation and 420-nm short-pass filter detection) and TPEF (840-nm excitation and broadband detection—between 400 and 700 nm) conditions. To further investigate this behavior, we fully suppressed the second-harmonic signal, using excitation at 850 nm and narrowband detection at 450 ± 5 nm. Even then, the polarization sensitivity of the TPEF signal to the polarization of the excitation light was clearly seen (see Fig. 14 presenting a part of *P. christiani* antenna recorded at two orthogonal polarization states). We observed that the signal can be significantly altered, and the SNR can be affected by simply rotating the polarization plane. Such behavior is not frequently observed, and it is not clear why this happens. However, according to Refs. 39 and 40, this behavior can be used to discriminate between different features or processes.

In this and similar studies, high-power femtosecond lasers are used. In our case, only a fraction of the available laser power was necessary for NLM of chitinous structures. By simply increasing the laser power (above 20 to 30 mW at the

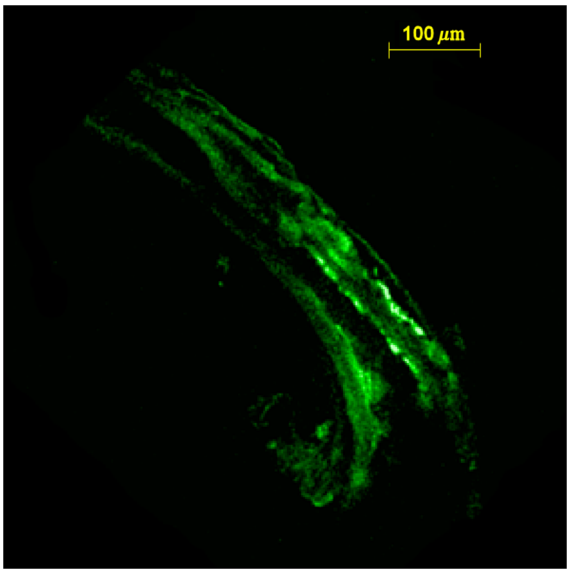

Fig. 12 Image of the inner sac of *P. ninae* aedeagus obtained upon 1040-nm excitation and broadband detection. Different structures are seen, as compared with Fig. 11(d).

sample), we were able to vaporize certain sections of cuticle and reveal internal, otherwise invisible, structures. This kind of tissue surgery has to be done carefully in order to localize laser-induced damage. This will be the subject of our further investigations.

There are several experimental problems that should be carefully treated when imaging insects. Samples should be kept in a mounting medium which is free of autofluorescence. We found that glycerin is more appropriate then Canada balsam, which has a high level of autofluorescence. In order to increase the penetration depth of the laser light, insects like *P. ninae* were initially soaked in clove oil, which clears the tissues to some degree. We have found no significant autofluorescence of clove oil and we are not aware of altered autofluorescence properties of the sample after the treatment.

In this study, we used only dead insects, but it is possible to work with live specimens, too, as verified in our experiments. If the power density is properly controlled, we have found that the laser radiation is not harmful, even for such sensitive tissues as insect compound eyes. We have observed *in vivo* ommatidia of several insects without the damaging effects of the laser light. This will be the subject of our future research.

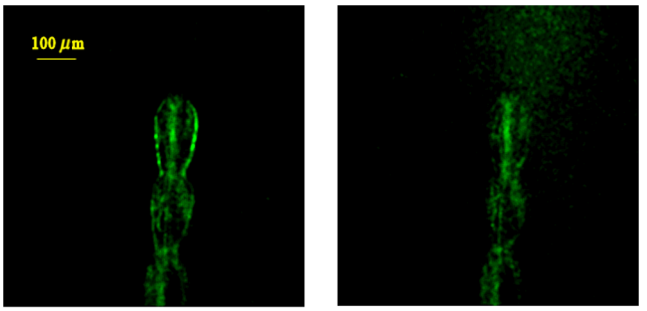

Fig. 14 The tip of *P. Christiani* antenna recorded at two orthogonal polarization states. (a) Horizontal polarization, (b) vertical polarization of excitation light.

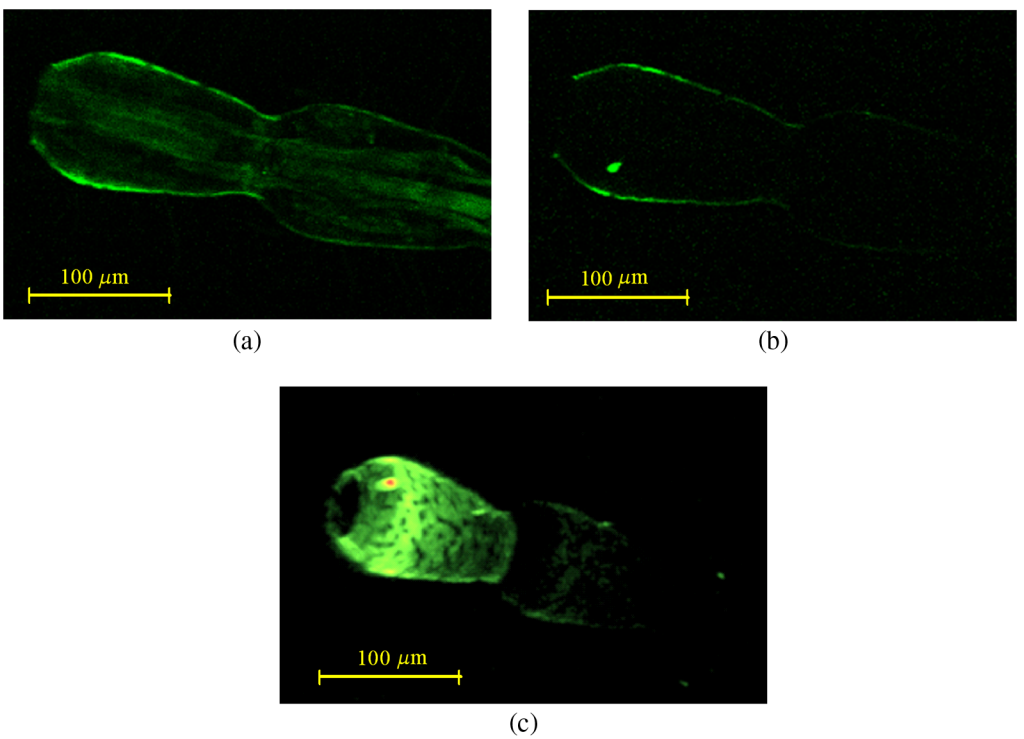

Fig. 13 The tip of *P. christiani* antenna, recorded by: (a) excitation at 840 nm and broadband detection between 400 and 700 nm (single slice); (b) excitation at 840 nm and narrow-band detection at 420 nm (single slice); and (c) volume rendering of the stack recorded under 840 nm excitation and 420 nm detection conditions.

6 Conclusions

We have shown that NLM is an efficient tool to study the morphology and anatomy of chitinous insect structures. It is a powerful technique that does not require tissue staining (as in confocal microscopy) or special tissue clearing methods (e.g., in selective plane illumination microscopy). Biological samples can be observed both *in vivo* and *in vitro*, with high resolution, quickly and without complicated preparation procedures. The autofluorescence spectrum and fluorescence time of chemically purified chitin were measured and the SHG signal was detected. Strong, two-photon excited autofluorescence and weaker SHG signals were used for imaging the insects. Exterior (head and antenna) and interior (male genitalia) body parts of two selected, cave-dwelling, insect species were studied and results were presented. A set of slices was recorded with a penetration depth of up to 200 μm. Many other insect species were analyzed, proving the universal applicability of the technique. We have found that almost any part of the insect body fluoresces. TPEF seems more suited to reflection analysis of whole insects, while SHG is more appropriate to transmission visualization of thin organs and structures like antennas and other appendages. NLM can also be used for dimensional metrology of an insect body and 3-D visualization of the body parts.

Apart from insects, the results of our study are applicable to a wide range of other biological taxa possessing chitin (algae, fungi, mollusks, other arthropods, and so on). Thanks to the high-penetration depth, NLM could enable studying of both morphological (external) and anatomical (internal) structures of a variety of living organisms. Such analyses are possible without any sample destruction or dissecting. The additional advantage of the technique is that either dead or living biological models could be experimentally observed.

Acknowledgments

The study was financially supported by the Serbian Ministry of Education, Science, and Technological Development (Projects Nos. ON171038, III45016, and ON173038). We also acknowledge FNSNF Scopes project, JRP IZ7370_127942. We are indebted to Mr. Dragan Antić (Institute of Zoology, University of Belgrade—Faculty of Biology, Belgrade, Serbia), who kindly allowed us to include his two photographs in the current paper. We express our gratitude to Dr Dragutin Šević (Institute of Physics, University of Belgrade, Serbia) for his help in establishing fluorescence time and fluorescence spectrum of chemically purified chitin. We thank to the personel of the Center for Laser Microscopy, University of Belgrade—Faculty of Biology, Belgrade, Serbia and Professor Pavle Andjus for enabling us to use their microscope objectives. Also, we would like to thank George Tserevelakis (Technical University of Munich, Germany and Institute of Electronic Structure and Lasers, Foundation for Research and Technology Hellas, Heraklion, Greece) for useful discussion and advices about the manuscript and the data processing.

References

1. P. T. C. So et al., "Two-photon excitation fluorescence microscopy," *Annu. Rev. Biomed. Eng.* **2**, 399–429 (2000).
2. J. L. Capinera, *Encyclopedia of Entomology*, 2nd ed., Springer, Dordrecht (2008).
3. J. Michels and S. N. Gorb, "Detailed three-dimensional visualization of resilin in the exoskeleton of arthropods using confocal laser scanning microscopy," *J. Microsc.* **245**, 1–16 (2012).
4. H. F. Nijhout, "The developmental physiology of color patterns in Lepidoptera," *Adv. Insect Physiol.* **18**, 181–247 (1985).
5. P. B. Koch et al., "Insect pigmentation: activities of β-alanyldopamine synthase in wing color patterns of wild-type and melanic mutant swallowtail butterfly *Papilio glaucus*," *Pigm. Cell Res.* **13**(Suppl 8), 54–58 (2000).
6. H. Peisker, J. Michels, and S. N. Gorb, "Evidence for a material gradient in the adhesive tarsal setae of the ladybird beetle *Coccinella septempunctata*," *Nat. Commun.* **4**, 1661 (2013).
7. G. Cárdenas et al., "Chitin characterization by SEM, FTIR, XRD, and 13C cross polarization/mass angle spinning NMR," *J. Appl. Polym. Sci.* **93**, 1876–1885 (2004).
8. H. L. Leertouwer, B. D. Wilts, and D. G. Stavenga, "Refractive index and dispersion of butterfly chitin and bird keratin measured by polarizing interference microscopy," *Opt. Express* **19**, 24061–24066 (2011).
9. B. de Campos Vidal, "Butterfly scale form birefringence related to photonics," *Micron* **42**, 801–807 (2011).
10. J. Michels, "Confocal laser scanning microscopy: using cuticular autofluorescence for high resolution morphological imaging in small crustaceans," *J. Microsc.* **227**, 1–7 (2007).
11. C.-H. Chien et al., "Label-free imaging of *Drosophila in vivo* by coherent anti-Stokes Raman scattering and two-photon excitation autofluorescence microscopy," *J. Biomed. Opt.* **16**, 016012 (2011).
12. D. E. Azofeifa, H. J. Arguedas, and W. E. Vargas, "Optical properties of chitin and chitosan biopolymers with application to structural color analysis," *Opt. Mater.* **35**, 175–183 (2012).
13. J. D. Schiffmann and C. L. Schauer, "Solid state physics characterization of α-chitin from *Vanessa cardui* Linnaeus wings," *Mater. Sci. Eng. C* **29**, 1370–1374 (2009).
14. G. Luna-Bárcenas et al., "FEMO modelling of optical properties of natural biopolymers chitin and chitosan," *Phys. Status Solidi (C)* **5**, 3736–3739 (2008).
15. K. Kumazawa and H. Tabata, "A three-dimensional fluorescence analysis of the wings of male *Morpho sulkowskyi* and *Papilio xuthus* butterflies," *Zool. Sci.* **18**, 1073–1079 (2001).
16. J. M. Gallas and M. Eisner, "Fluorescence of melanin-dependence upon excitation wavelength and concentration," *Photochem. Photobiol.* **45**, 595–600 (1987).
17. M. Brydegaard et al., "Insect monitoring with fluorescence lidar techniques: feasibility study," *Appl. Opt.* **48**, 5668–5677 (2009).
18. K. Christiansen, "Morphological adaptations," in *Encyclopedia of Caves*, W. B. White and D. C. Culver, Eds., 2nd ed., pp. 517–528, Elsevier, Amsterdam (2012).
19. D. C. Culver and T. Pipan, *The Biology of Caves and Other Subterranean Habitats*, Oxford University Press, Oxford (2009).
20. I. Ribera et al., "Ancient origin of a Western Mediterranean radiation of subterranean beetles," *BMC Evol. Biol.* **10**, 1–14 (2010).
21. G. Filippidis et al., "Imaging of *Caenorhabditis elegans* neurons by second-harmonic generation and two-photon ex-citation fluorescence," *J. Biomed. Opt.* **10**, 024015 (2005).
22. W. Supatto et al., "*In vivo* modulation of morphogenetic movements in *Drosophila* embryos with femtosecond laser pulses," *Proc. Natl. Acad. Sci. U. S. A.* **102**, 1047–1052 (2005).
23. D. Debarre et al., "Imaging lipid bodies in cells and tissues using third-harmonic generation microscopy," *Nat. Methods* **3**, 47–53 (2006).
24. C. Y. Lin et al., "Label-free imaging of *Drosophila* larva by multiphoton autofluorescence and second harmonic generation microscopy," *J. Biomed. Opt.* **13**, 050502 (2008).
25. J.-A. Conchello and J. W. Lichtman, "Optical sectioning microscopy," *Nat. Methods* **2**, 920–931 (2005).
26. B. Condé and C. Bareth, "Une évolution de *Stygiocampa*, sous-genre troglomorphe de *Plusiocampa* (Diplura Campodeidae), avec la description d'une nouvelle espèce de Serbie orientale," *Rev. Suisse Zool.* **103**, 369–381 (1996).
27. J. Pages, "Remarks on the Japygidae (Insecta, Diplura) reported for the underground environment," *Int. J. Speleol.* **1**, 192–201 (1964).
28. A. I. Camacho, *The Natural History of Biospeleology*, Monografias del Museo nacional de ciencias naturals, Consejo superior de investigaciones científicas, Madrid (1992).
29. S. B. Ćurčić et al., "On a new cave-dwelling beetle (Trechinae, Carabidae) from Serbia," *Arch. Biol. Sci.* **56**, 109–113 (2004).

30. M. Moseley, "Observations on the cave-associated beetles (Coleoptera) of Nova Scotia, Canada," *Int. J. Speleol.* **38**, 163–172 (2009).
31. J. B. Guild, C. Xu, and W. W. Webb, "Measurement of group delay dispersion of high numerical aperture objective lenses using two-photon excited fluorescence," *Appl. Opt.* **36**, 397–401 (1997).
32. W. Denk, J. H. Strickler, and W. W. Web, "Two-photon laser scanning fluorescence microscopy," *Science* **248**, 73–76 (1990).
33. O. T. Moldovan, "Beetles," in *Encyclopedia of Caves*, W. B. White and D. C. Culver, Eds., 2nd ed., pp. 54–62, Elsevier, Amsterdam (2012).
34. P. J. Gullan and P. S. Cranston, *The Insects: An Outline of Entomology*, John Wiley & Sons, New York (2009).
35. B. Nie et al., "Multimodal microscopy with sub-30 fs Yb fiber laser oscillator," *Biomed. Opt. Express* **3**, 1750–1756 (2012).
36. E. J. Gualda et al., "*In vivo* imaging of anatomical features of the nematode *Caenorhabditis elegans* using non-linear (TPEF-SHG-THG) microscopy," *Proc. SPIE* **6630**, 663003 (2007).
37. R. Carriles et al., "Imaging techniques for harmonic and multiphoton absorption fluorescence microscopy," *Rev. Sci. Instrum.* **80**, 081101 (2009).
38. C. K. Chou et al., "Polarization ellipticity compensation in polarization second-harmonic generation microscopy without specimen rotation," *J. Biomed. Opt.* **13**, 014005 (2008).
39. T. Parasassi et al., "Two-photon microscopy of aorta fibers shows proteolysis induced by LDL hydroperoxides," *Free Radical Biol. Med.* **28**, 1589–1597 (2000).
40. Q. Yua and A. A. Heikal, "Two-photon autofluorescence dynamics imaging reveals sensitivity of intracellular NADH concentration and conformation to cell physiology at the single-cell level," *J. Photochem. Photobiol., B* **95**, 46–57 (2009).

Mihailo D. Rabasović is a research associate at the Institute of Physics, University of Belgrade, Serbia. He received his PhD degree in physics from the Physics Department of the University of Belgrade in 2007. His current research interests include photoacoustics, microscopy, and correlation spectroscopy.

Dejan V. Pantelić is a senior researcher at the Institute of Physics, University of Belgrade, Serbia. He received his PhD degree in optics from the Physics Department of the University of Belgrade in 1990. His current research interests include biophotonics, microscopy, and holography. He is a member of OSA.

Branislav M. Jelenković is a research professor at the Institute of Physics, University of Belgrade, Serbia. He received his PhD degree in atomic physics in 1983. His current research interests include laser spectroscopy, quantum and nonlinear optics, and biophysics. He is current president of optical society of Serbia and the member of OSA.

Srećko B. Ćurčić is an associate professor at the Institute of Zoology, University of Belgrade—Faculty of Biology, Serbia. He received his PhD degree in morphology, systematics, and phylogeny of animals from the Institute of Zoology, University of Belgrade—Faculty of Biology, in 2005. His current research interests include morphology, systematics, taxonomy, phylogeny, development and ecology of the Coleoptera order (Insecta), diversity and faunistics of both soil- and cave-dwelling invertebrates, and defensive secretion in ground beetles. He is a member of numerous scientific societies.

Maja S. Rabasović is a research associate at the Institute of Physics, Belgrade, Serbia. She received her PhD degree from the Physics Department of the University of Belgrade, in 2013. Her current research interests include electron atom collision processes, laser-induced fluorescence, and laser-induced breakdown spectroscopy.

Maja D. Vrbica is a research assistant at the Institute of Zoology, University of Belgrade—faculty of biology, Serbia. Her current research interests include morphology, taxonomy, systematic, and phylogeny of some ground beetles (Insecta, Coleoptera).

Vladimir M. Lazović is a research assistant at the Institute of Physics, University of Belgrade, Serbia. His research interests include electron microscopy, nonlinear microscopy, optics, and lasers.

Božidar P. M. Ćurčić is a full professor at the Institute of Zoology, University of Belgrade—Faculty of Biology, Serbia. He received his PhD degree in morphology, systematics, phylogeny, and development of animals from the Department of Zoology, University of Belgrade—Faculty of Science, in 1976. His current research interests include morphology, systematics, taxonomy, phylogeny, and developmental biology of Arthropoda. He is the corresponding member of Bulgarian Academy of Sciences, member or fellow of 25 international societies, and president of MAB UNESCO Serbia.

Aleksandar J. Krmpot is a research associate at the Institute of Physics, University Belgrade, Serbia, and guest researcher at the Karolinska Institute, Stockholm, Sweden. He received his PhD degree in physics (quantum optics) from the Physics Department of the University of Belgrade. His current research interests are coherent laser spectroscopy and quantum optics, nonlinear microscopy, and correlation spectroscopy.